Received: 11 April 2017 | Revised: 3 May 2017 | Accepted: 4 May 2017

DOI: 10.1002/poc.3720

SPECIAL ISSUE ARTICLE

WILEY Journal of Physical Organic Chemistry

Functionalization of oxabenzonorbornadiene: Manganese(III)-mediated oxidative addition of dimedone†

Raşit Çalışkan[1,2] | Ozlem Sari[2,3] | Metin Balci[2]

[1]Department of Chemistry, Süleyman Demirel University, Isparta, Turkey

[2]Department of Chemistry, Middle East Technical University, Ankara, Turkey

[3]Department of Chemistry, Ahi Evran University, Kırşehir, Turkey

Correspondence
Raşit Çalışkan and Metin Balci, Department of Chemistry, Middle East Technical University, 06800 Ankara, Turkey.
Email: rasitcaliskan@sdu.edu.tr; mbalci@metu.edu.tr

Funding information
Middle East Technical University (METU); Turkish Academy of Sciences (TUBA)

Abstract

3-Chloro-1,2,3,4-tetrahydro-1,4-epoxynaphthalen-2-yl)-3-hydroxy-5,5-dimethylcyclohex-2-en-1-one, synthesized by the reaction of oxabenzonorbornadiene with $Mn(OAc)_3$ and dimedone in the presence of HCl in acetic acid, was submitted to ring-opening reactions with BBr_3 and H_2SO_4. Reaction with BBr_3 yielded 2 products, a 5-membered ring and an 8-membered ring, with the former being the major product. However, the H_2SO_4-supported reaction exclusively formed an 8-membered ring. The mechanism of formation of these products was supported by theoretical calculations.

KEYWORDS

cycloaddition, dimedone, manganese(III) acetate, oxabenzonorbornadiene, rearrangement, ring-opening reaction

1 | INTRODUCTION

Heterobicyclic alkenes such as 7-oxabicyclo[2.2.1]heptanes, 7-oxabicyclo-[2.2.1]heptenes, and their benzo derivatives (**1-3**) are valuable intermediates in the total synthesis of some natural products and analogues.[1] These 7-oxanorbornane derivatives can be easily synthesized through Diels-Alder addition of furans to alkenes or benzynes.

1

2

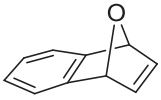

3

The ring-opening chemistry of oxabicyclic compounds underwent significant growth in recent decades and so the oxabicyclic template has become increasingly common as a starting material in the preparation of both cyclic and acyclic compounds. A crucial synthetic transformation using these intermediates involves the cleavage of the bridging carbon–oxygen bond in these systems to produce functionalized cyclohexenes or cyclohexenols. The ring-opening reactions can be triggered by acid catalysts,[2] bases,[3] and metals.[4]

For example, nucleophilic ring-opening of 7-oxabenzonorbornadiene (**3**) provides different substituted dihydronaphthalenol derivatives, depending on the catalysts and nucleophiles.[4g]

The ring-opening reaction of 7-oxabenzonorbornene (**3**) with phenyl iodide in the presence of Pd/BINAP catalyst results in the formation of **4** and **5** (3:2 ratio) with *cis* configuration in 85% yield (Scheme 1).[4g] Allylation of 7-oxabenzonorbornane derivatives was achieved with potassium trifluoroborate in the presence of some metal catalysts. Using $CoBr_2$ mainly gave the ring-opening product **7**.[4a] An interesting feature of these products is their *syn* configuration. In the case of nucleophilic ring-opening reactions, the nucleophile can attack at the bridgehead carbon atom with simultaneous cleavage of the C−O bond to give the ring-opening product **8**. The position of the double bond is retained after the ring-opening process (Scheme 2). On the other hand, an S_N2' nucleophilic attack on the double bond

†This article is published as part of a special issue to celebrate the 80th birthday of Professor Waldemar Adam

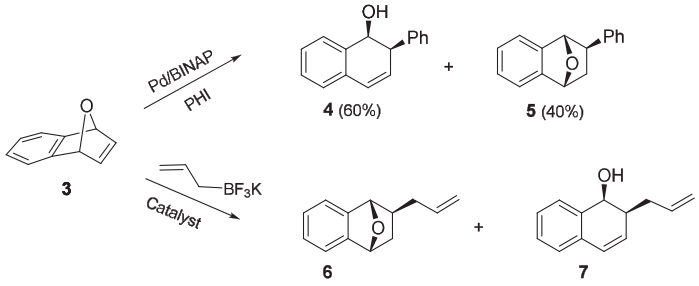

SCHEME 1 Metal-catalyzed ring-opening reaction of oxabenzonorbornadiene (**3**) with nucleophiles

would generate the rearranged compound **9** with *cis* configuration.

In this paper, we describe the BBr_3-catalyzed ring-opening reaction of **13** synthesized by the reaction of 7-oxabenzonornadiene (**3**) with dimedone in the presence of $Mn(OAc)_3$ and HCl.

2 | RESULTS AND DISCUSSION

Very recently, we were interested in the addition mechanism of 1,3-dicarbonyl compounds to double bonds in the presence of $Mn(OAc)_3$.[5,6] In particular, we chose bicyclic systems, which have great tendency for rearrangement. When the reaction of oxabenzonorbornadiene (**3**) with dimedone (**10**) was conducted in the presence of $Mn(OAc)_3$ in acetic acid, the rearranged products **11** and **12** were formed in 56% and 14% yields, respectively (Scheme 3).

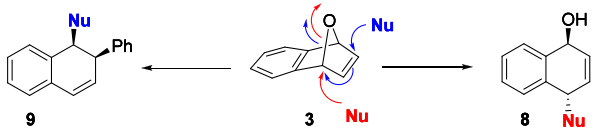

SCHEME 2 Mechanism of the ring-opening reaction of oxabenzonorbornadiene (**3**) with nucleophiles

The formation of the rearranged products was not expected because 7-oxabenzonorbornadiene (**3**) mainly undergoes a ring-opening reaction upon treatment with electrophiles.[3,7] We assume that the initially formed cation undergoes Wagner-Meerwein type rearrangement, thus forming a new cation that is captured by the oxygen atom of the carbonyl group in **10** to form **12**. To hinder the Wagner-Meerwein type rearrangement, we decided to run the same reaction in the presence of HCl so that the initially formed cation can be captured by the chloride ion present in the reaction media.

The reaction of oxabenzonorbornadiene **3** with dimedone (**10**) and $Mn(OAc)_3$ in the presence of HCl in acetic acid gave the adduct **13** in 82% yield (Scheme 3). Careful examination of the reaction mixture did not reveal the formation of any trace of rearranged products. The structure of **13** was unambiguously determined by NMR spectral data. The *exo* configuration of the chlorine atom and dimedone ring was confirmed by measuring the coupling constants between H-1 and H-2 and between H-3 and H-4. The absence of any coupling between the relevant protons confirms exclusively the *endo*

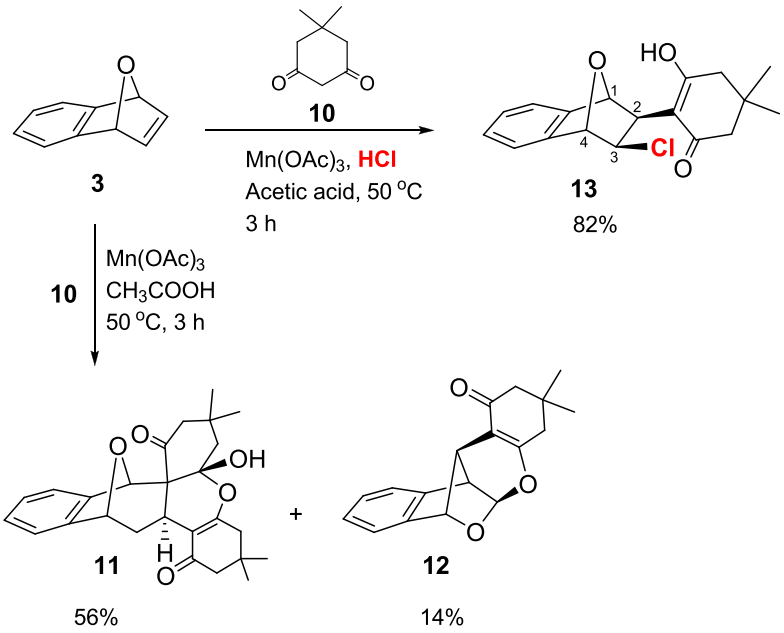

SCHEME 3 The reaction of oxabenzonorbornadiene **3** with $Mn(OAc)_3$ in the presence and absence of HCl

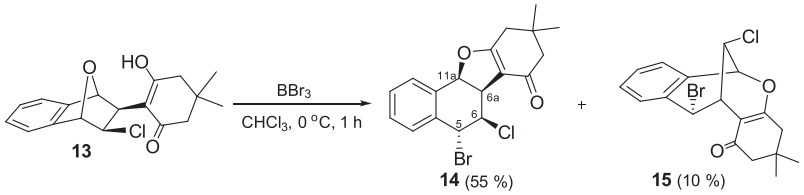

SCHEME 4 The reaction of the adduct **13** with BBr_3 in dichloromethane

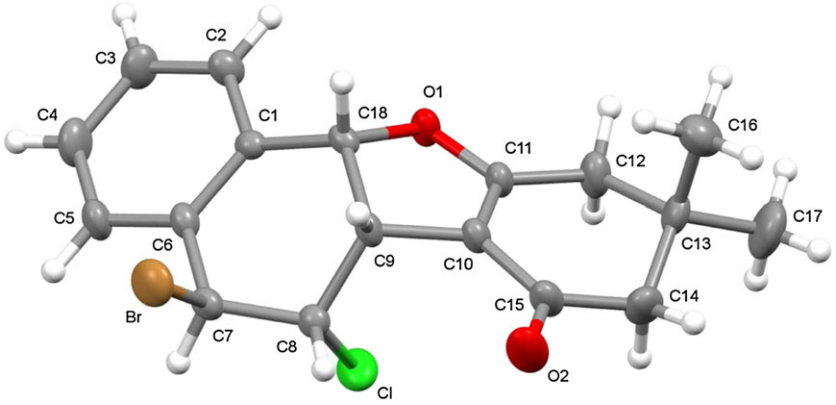

FIGURE 1 X-ray crystal structure of **14**

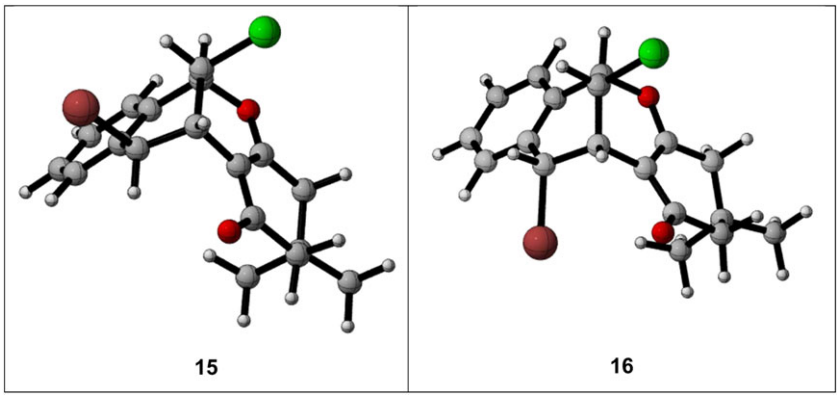

FIGURE 2 Geometry optimized structures of **15** and **16**

TABLE 1 The dihedral angles, measured coupling constants, and calculated coupling constants for **15** and **16**

	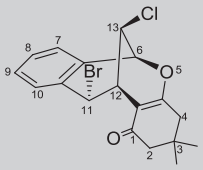			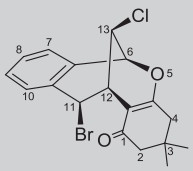	
	15			16	
	Dihedral Angle	**Coupling Constant Calculated, Hz**	**Coupling Constant Experimental, Hz**	**Dihedral Angle**	**Coupling Constant Calculated, Hz**
H-C11-C12-H	65.6°	**2.3**	2.6	44.5 °	**5.0**
H-C12-C13-H	69.6°	2.0	2.3	68.5 °	2.1
H-C13-C6-H	60.0 °	3.5	2.3	62.2 °	3.30

orientation of the protons H-2 and H-3. In the case of *exo* orientation of these protons, a high value of $J_{1,2}$ and $J_{3,4}$, 3.5-5.0 Hz, would be expected.[7,8] Furthermore, 2 resonance signals in the ^{13}C-NMR spectrum appearing at 196.7 and 173.8 ppm clearly indicate that one of the carbonyl groups exists in its enol form.[9] Otherwise, the resonance frequencies of the carbonyl groups would appear at higher than 200 ppm. The formation of **13** was rationalized by a fast intramolecular capture of the cation formed after the addition of dimedone radical to the double bond followed by oxidation.

For further functionalization of the oxanorbornene unit, the adduct **13** was submitted to a BBr_3-mediated ring-opening reaction. The reaction of **13** with BBr_3 in dichloromethane gave 2 separable products, the ring-opening products **14** and **15** in 55% and 10% yields, respectively (Scheme 4). Inspection of the proton nuclear magnetic resonance spectra spectra of those compounds showed the presence of 2 constitutional isomers.

Geometry optimization calculations (M06[10]/6-311G +(d,p) level in gas phase) for **14** show dihedral angles of 19.1°, 48.9°, and 58.3° between the vicinal protons H-11a/H-6, H-6a/H-6, and H-6/H-5, respectively. We calculated the vicinal coupling constants between the relevant protons considering substituent electronegativities and found values of 7.8, 4.4, and 2.5 Hz, respectively.[11] The experimentally measured coupling constants of 10, 3.1, and 3.1 Hz are in good agreement with the proposed structure. Finally, the structure of **14** was further confirmed by X-ray crystallographic analysis showing the *cis* configuration of the dihydrofurane ring. (Figure 1).

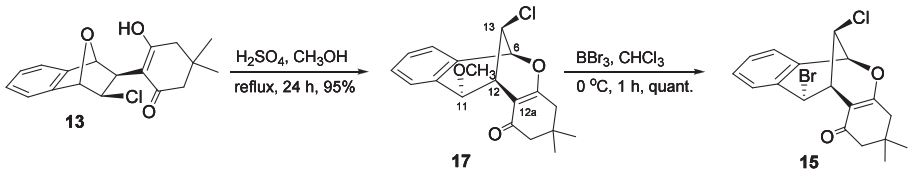

SCHEME 5 Ring-opening reaction of **13** with H_2SO_4

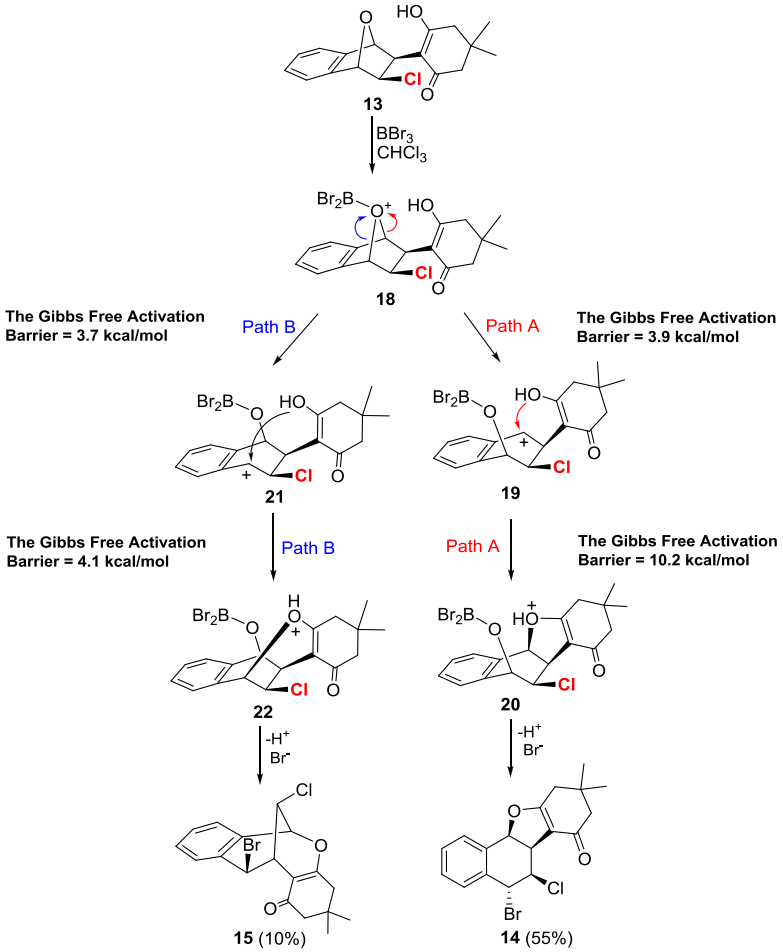

SCHEME 6 BBr_3 activated ring opening reaction mechanism for the formation of **14** and **15**

The structure of the isomer **15** was assigned based on its NMR spectra and geometry optimization calculations (M06[10]/6-311G+(d,p) level in gas phase) (Figure 2). First, we determined the constitution of the molecule. To assign the correct configuration (*exo* or *endo*) of the bromine atom in **15,** the dihedral angles for the vicinal protons H-C11-C12-H, H-C12-C13-H, and H-C13-C6-H were calculated using the geometry optimized structures **15** and **16**.[11]

The measured coupling constants and the calculated coupling constants are given in Table 1. The measured coupling constant, $J_{11,12} = 2.3$ Hz, in **15** is in good agreement with the calculated one, $J_{11,12} = 2.0$ Hz. In the case of the *endo* orientation of the bromine atom in **16**, the calculated dihedral angle is 44.5°. Here, one would expect a larger coupling constant of $J \approx 5.0$ Hz. On the basis of these coupling constants, the *exo* configuration was assigned to the bromine atom in **15**. Furthermore, we found that the *exo* isomer **15** is thermodynamically 5.1 kcal/mol more stable than the *endo* isomer **16**.

We then examined the scope of the ring-opening reaction for **13** with H_2SO_4 in methanol. A solution of **13** in methanol was treated with H_2SO_4 at 0°C (Scheme 5). The regioselective ring-opening product **17** was isolated as the sole isomer. Treatment of **17** with BBr_3 as described above resulted in the exclusive formation of **15** with configuration retention in quantitative yield.

The structure of **17** was determined with the help of 1D (^{1}H- and ^{13}C-) and 2D (COSY, HSQC, and HMBC) NMR spectra. The HMBC spectrum shows that the carbon signal resonating at 81.9 (C-11) ppm correlates with the aromatic protons as well as with methoxy protons appearing at 3.41 ppm. This finding clearly shows that the methoxy group is bonded to the carbon atom C-11. Furthermore, the double bond carbon atom (C-12a) resonating at high field (107.5 ppm) correlates with the proton resonances of H-11, H-12, and H-13 and with the methylene protons in the ring. This is in complete agreement with the suggested structure **17**. The configuration of the methoxy group was again assigned by measuring the coupling constant between the

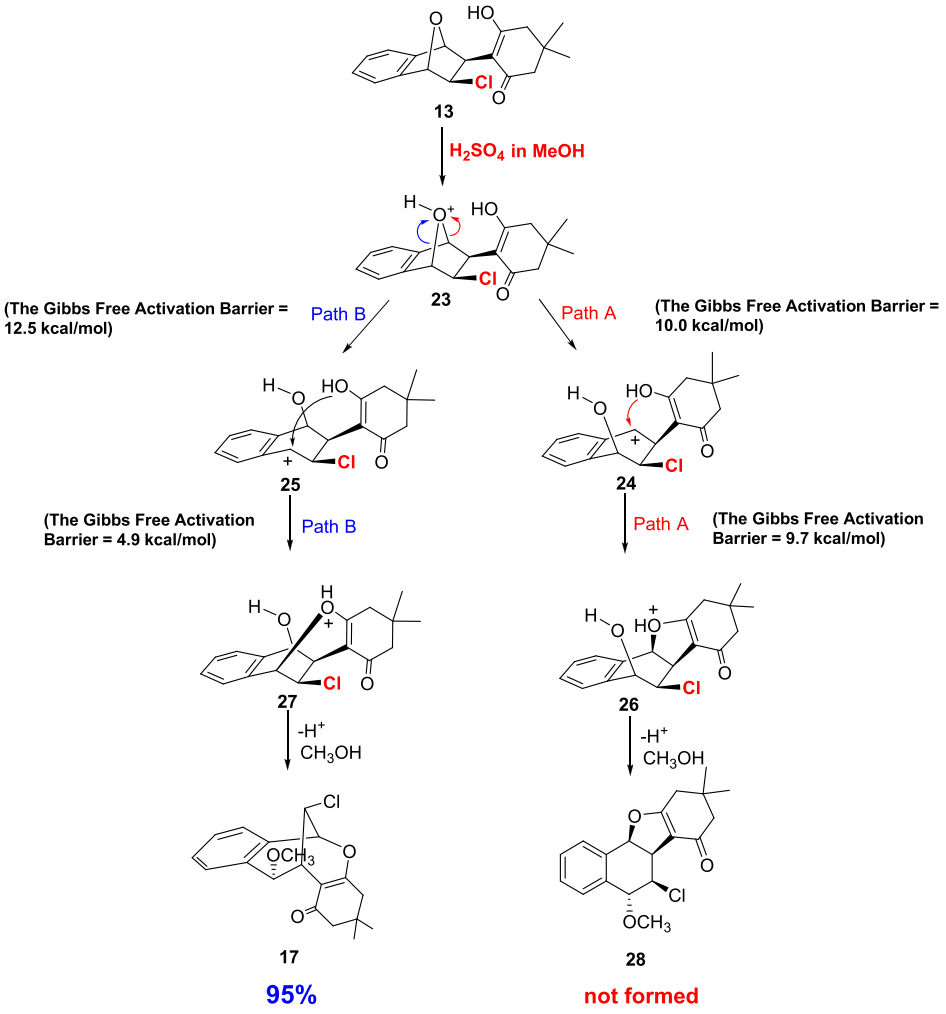

SCHEME 7 Proposed mechanism for the formation of **17**

vicinal protons H11-C-C-H12, and it was found that this coupling is 2.6 Hz, exactly the same value as determined by **15**. Therefore, we assigned the *exo* configuration to the methoxy group in **17**.

The reaction of methoxy compound **17** with BBr_3 in chloroform under the same reaction conditions as shown in Scheme 4 gave **15** in almost quantitative yield. The configuration at the C-11 carbon atom was retained. We assume that the first step is the removal of the methoxy group to form a benzylic cation that can be exclusively captured from the *exo* face of the cation as the *endo* face is partially blocked by the dimedone group. On the other hand, geometry optimization calculations showed that the *exo* isomer **15** is 5.1 kcal/mol more stable than the *endo*

TABLE 2 Optimized geometries of the stationary points of the formation of **19** and **21**. Distances are given in angstroms

PATH A		
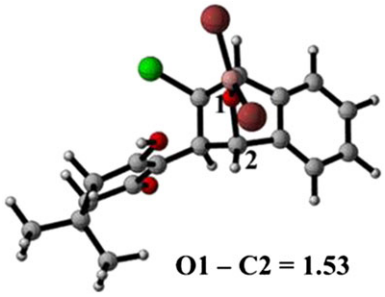 **18**	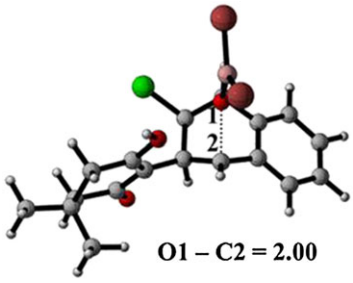 **TS1**	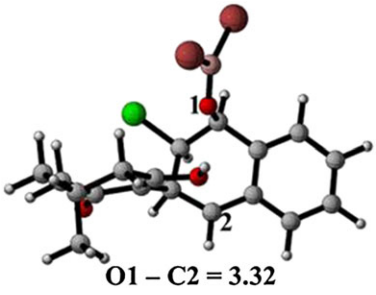 **19**
PATH B		
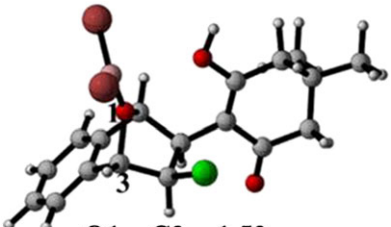 **18**	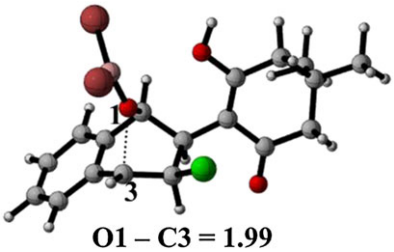 **TS2**	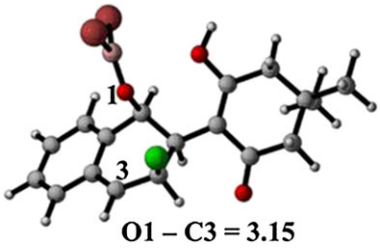 **21**

TABLE 3 Optimized geometries of the stationary points of the formation of **24** and **25**. Distances are given in angstroms

PATH A		
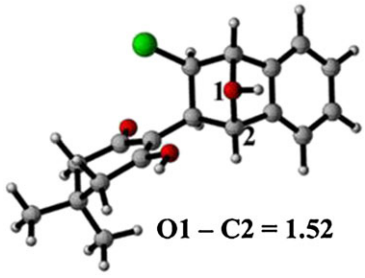 **23**	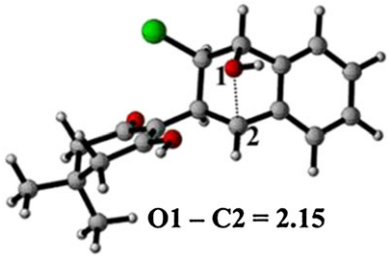 **TS3**	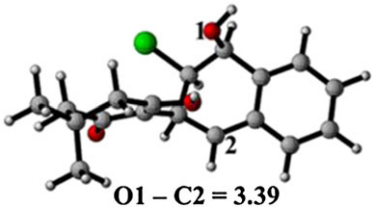 **24**
PATH B		
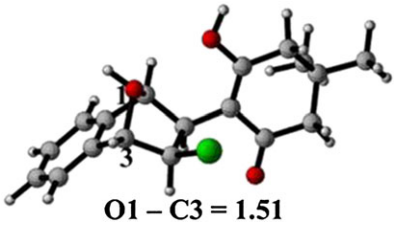 **23**	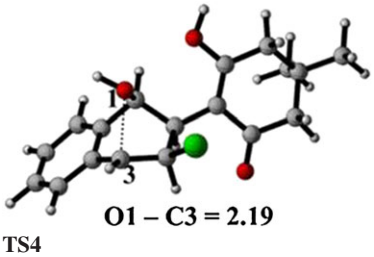 **TS4**	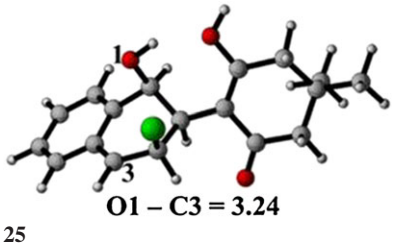 **25**

TABLE 4 Optimized geometries of the stationary points of the formation of **19** and **20**. Distances are given in angstroms. In path B, hydrogen atoms are omitted for clarity

PATH A		
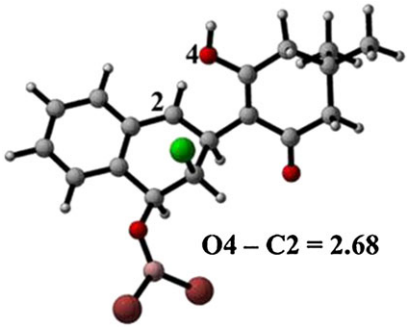	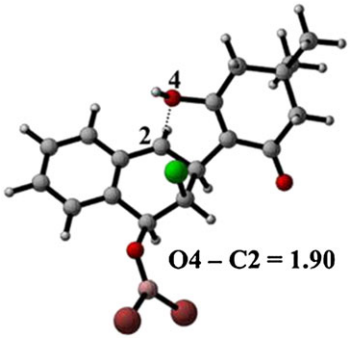	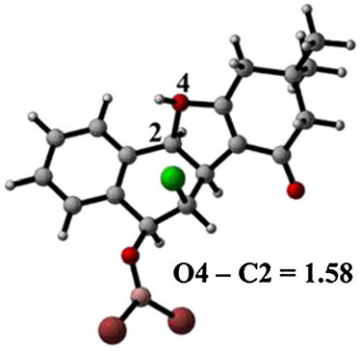
19	**TS5**	**20**
PATH B		
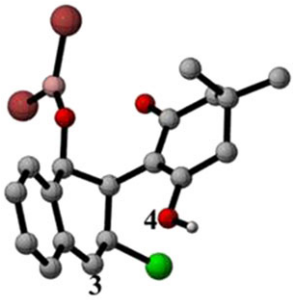	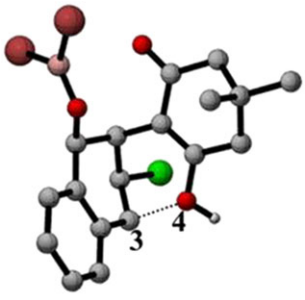	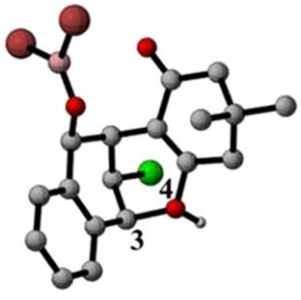
21	**TS6**	**22**

TABLE 5 Optimized geometries of the stationary points of the formation of **26** and **27**. Distances are given in angstroms. In path B, hydrogen atoms are omitted for clarity

PATH A		
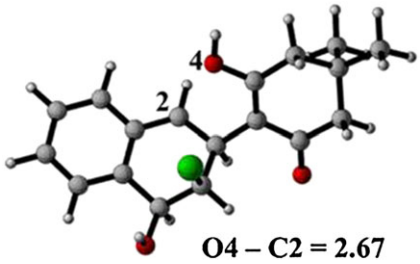	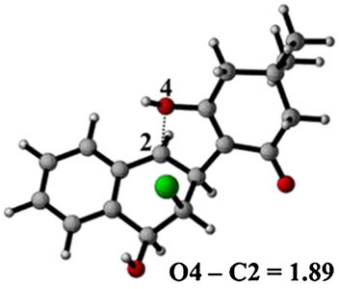	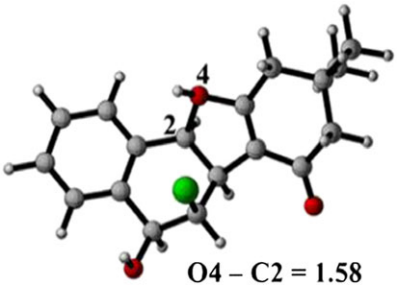
24	**TS7**	**26**
PATH B		
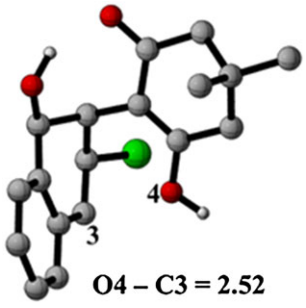	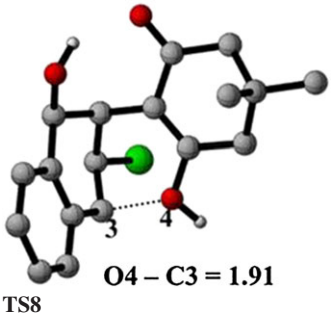	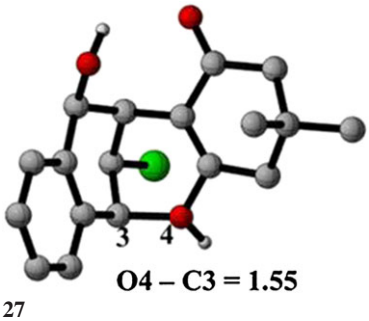
25	**TS8**	**27**

isomer. Therefore, we assume the thermodynamic stability of the *exo*-isomer is also the driving force for the exclusive formation of the *exo*-isomer **17**.

3 | METHODOLOGY

All computations were performed using the Gaussian 09[12] software package. The geometries of all the reactants, transition states, intermediates, and products were fully optimized by using ωB97XD[13]/6-31G+(d,p) with the conductor-like polarizable continuum solvation model[14] in methanol or chloroform, except otherwise indicated. Frequency calculations were performed at the same level of theory to verify whether the structures are minima or transition states. Thermodynamic calculations were conducted at 25°C and 1 atm. Structural representations were generated using CYLview.[15]

Herein, we attempted to explore the regioselective ring-opening reaction mechanism of compound **13** by means of density functional theory calculations, and the results obtained from both mechanisms were compared to understand the experimentally observed product distribution.

For this regioselective ring-opening process of **13**, we suggest the following reaction mechanism (Schemes 6 and 7). The first step is the coordination of boron tribromide to the bridge oxygen atom to form the zwitter-ionic intermediate **18**. There are 2 possible modes of ring-opening for the intermediate **18**; paths A and B.

The calculated Gibbs free energy barriers for ring-opening reactions of paths A and B are 3.9 and 3.7 kcal/mol, respectively, which demonstrates, that kinetically, both paths are almost identical. The optimized structures are depicted in Table 2. In path A, O1-C2 distance is lengthened from 2.00 Å in transition state **TS1** to 3.32 Å in **19**. On the other hand, in path B, the distance of O1-C3 is lengthened from 1.99 Å in transition state **TS2** to 3.15 Å in **21**. Calculations show that the carbocation **19** formed in path A is 6.9 kcal/mol more stable than the carbocation **21** formed in path B. This may be due to the inductive effect of the chlorine, which destabilizes the cationic intermediate **21**. In addition, interaction between the hydroxyl oxygen atom and positively charged C2 (the distance is 2.68 Å) contributes to the stability of the intermediate **19**. This energy difference is in agreement with the experimental observation that the major product **14** is formed by the most stable intermediate.

Similarly, the first step of the reaction of **13** using H_2SO_4 was also investigated. The computed activation barriers for paths A and B are 10.0 and 12.5 kcal/mol, respectively. The optimized structures are shown in Table 3.

Once the carbocations were formed, 2 probable pathways were proposed for the ring closure step, shown in Table 4. In path A, a nucleophilic attack of the hydroxyl oxygen atom on C2 carbon atom takes place via **TS5**. The Gibbs free activation barrier for this step is calculated to be 10.2 kcal/mol. On the other hand, in path B, nucleophilic attack of the hydroxyl oxygen atom on C3 carbon atom takes place via **TS6**. The calculated Gibbs free activation barrier for path B is 4.1 kcal/mol.

Similarly, the second step of the reaction of **13** with H_2SO_4 was also investigated. Optimized structures are depicted in Table 5. This step involves the nucleophilic attack of hydroxyl oxygen on either C2 or C3 carbon atoms. The Gibbs free energy barrier associated with transition state TS7 is 9.7 kcal/mol. On the other hand, the calculated Gibbs free activation energy for path B is only 4.9 kcal/mol, which is much lower than that of path A. TS7 could be unfavorable due to formation of a strained 5-membered ring instead of 8-membered ring. This energy difference is in agreement with the experimental observation.

4 | CONCLUSION

The reaction of oxabenzonorbornadiene **3** with dimedone (**10**) and $Mn(OAc)_3$ in the presence of HCl in acetic acid gave the adduct **13**. For further functionalization, **13** was submitted to a ring-opening reaction in the presence of BBr_3 and H_2SO_4. The BBr_3-supported ring-opening reaction of **13** resulted in the formation of a 5-membered ring **14** and **15** as the minor product. However, the ring-opening reaction with H_2SO_4 exclusively resulted in the formation of **17,** a bicyclic system that was further converted to **15** upon reaction with BBr_3. The structures were determined with the help of NMR spectra, and the mechanism of formation of the products was supported by theoretical calculations.

5 | EXPERIMENTAL SECTION

5.1 | General

Proton nuclear magnetic resonance spectra were recorded on a 400 MHz instrument. The ^{13}C NMR spectra were recorded on a 100 MHz instrument. Column chromatography was performed on silica gel (60 mesh). High-resolution mass spectra were recorded by LC-MS TOF electrospray ionization. Infrared (IR) spectra were recorded in the range 4000 to 600 cm^{-1} via attenuated total reflection diamond. Melting points were measured using a melting point apparatus and were uncorrected.

5.2 | Oxidative addition of dimedone (2) to 7-oxabenzonorbornadiene (3) in the presence of $Mn(OAc)_3$ and HCl

A solution of 7-oxabenzonorbornadiene (**3**) (0.72 g, 5.0 mmol) and dimedone (**10**) (0.7 g, 5.0 mmol) in

15 mL of glacial AcOH was added to a solution of $Mn(OAc)_3 \bullet 2H_2O$ (2.68 g, 10.0 mmol) and HCl (1 mL, 37 %) in 50 mL of glacial AcOH. The resulting mixture was stirred under N_2 at 50°C for 3 hours. When the reaction was complete, the solution was concentrated under reduced pressure and quenched with 100 mL saturated aqueous $NaHCO_3$ solution. The mixture was extracted with CH_2Cl_2. The combined organic layers were washed several times with H_2O and dried ($MgSO_4$). The chromatography of the residue on silica gel eluting with (hexane/EtOAc, 3:1) gave 1.3 g of **13** (82 %).

5.3 | 2-((1*S*,2*R*,3*R*,4*S*)-3-chloro-1,2,3,4-tetrahydro-1,4-epoxynaphthalen-2-yl)-3-hydroxy-5,5-dimethylcyclohex-2-enone (13)

Colorless crystals, mp 145 to 147°C; ^{1}H-NMR (400 MHz, $CDCl_3$) δ 10.03 (s, 1H), 7.37 to 7.24 (m, 4H), 5.58 (s, 1H), 5.41 (s, 1H), 4.30 (d, J = 7.6 Hz, 1H), 3.94 (d, J = 7.6 Hz, 1H), 2.51 (d, A part of AB system, J = 17.4 Hz, 1H), 2.44 (d, B part of AB system, J = 17.4 Hz, 1H), 2.28 (s, 2H), 1.12 (s, 6H); ^{13}C-NMR (100 MHz, $CDCl_3$) δ 196.7, 173.8, 144.2, 141.0, 128.8, 128.4, 120.7, 120.2, 111.3, 89.0, 84.2, 62.9, 50.5, 44.8, 41.3, 32.0, 29.1, 28.5; IR (KBr, cm^{-1}): 3511, 2925, 2910, 1722, 1684, 1397, 1365, 974, 936, 776, 716, 647; HRMS-TOF $[M + H]^+$: Calcd for $C_{18}H_{20}O_3Cl$: 319.1138, found: 319.1101.

5.4 | Reaction of 13 with BBr_3

Boron tribromide (1.94 mL, 5.05 g, 20.2 mmol) was added dropwise to a solution of **13** (0.31 g, 10 mmol in dry dichloromethane (25 mL) at 0°C. After 1 hour, the solution was concentrated under reduced pressure and quenched with 100 mL saturated aqueous $NaHCO_3$ solution. The mixture was extracted with CH_2Cl_2. The combined organic layers were washed several times with H_2O and dried ($MgSO_4$). The chromatography of the residue on silica gel (65.0 g) eluting with hexane/EtOAc (3:1) gave **15** (0.03 g, 10 %) as the first fraction. The isomer **14** (0.21 g, 55 %) was isolated as the second fraction.

5.5 | *rel*-(5*R*(*S*),6*R*(*S*),6a*R*(*S*),11a*S*(*R*))-5-bromo-6-chloro-9,9-dimethyl-6,6a,8,9,10,11a-hexahydro-naphtho[1,2-b]benzofuran-7(5*H*)-one (14)

Colorless crystals, mp 111 to 114°C; ^{1}H-NMR (400 MHz, $CDCl_3$) δ 7.62 to 7.36 (m, 4H), 5.32 (d, J = 10.0 Hz, 1H, H-11a) 5.45 (d, J = 3.1 Hz, 1H, H-5), 5.11 (t, J = 3.1 Hz, 1H, H-6), 4.45 (dd, J = 10.0 and 3.1 Hz, 1H, H-6a), 2.44 (dd, A part of AB system, J = 17.8 and 1.6 Hz, 1H, CH_2), 2.35 (d, A part of AB system, J = 16.1 Hz, 1H, CH_2), 2.33 (d, B part of AB system, J = 16.1 Hz, 1H, CH_2), 2.25 (d, B part of AB system, J = 17.8 Hz, 1H, CH_2), 1.17 (s, 3H, CH_3), 1.12 (s, 3H, CH_3); ^{13}C-NMR (100 MHz, $CDCl_3$) δ 194.1, 177.1, 132.9, 130.4, 129.7, 129.6, 129.2, 126.0, 113.5, 79.8, 57.7, 50.9, 47.8, 39.5, 37.7, 34.4, 29.5, 28.1; IR (KBr, cm^{-1}): 2958, 2865, 2124, 2748, 1722, 1637, 855, 749, 632, 518; HRMS-TOF $[M + H]^+$: Calcd for $C_{18}H_{19}O_2BrCl$ 381.0257, found: 381.0273.

5.6 | *rel*-(6*S*(*R*),11*R*(*S*),12*S*(*R*),13*R*(*S*))-11-bromo-13-chloro-3,3-dimethyl-2,3,4,6,11,12-hexa-hydro-1H-6,12-methanodibenzo[b,f] oxocin-1-one (15)

Colorless crystals, mp 127 to 129°C; ^{1}H-NMR (400 MHz, $CDCl_3$) δ 7.38 to 7.33 (m, 4H, arom.), 5.46 (d, J = 2.6 Hz, 1H, H-11), 5.29 (t, J = 2.3 Hz, 1H-6), 5.0 (t, J = 2.3 Hz, 1H, H-13), 3.64 (bs, 1H, H-12), 2.25 (d, A part of AB system, J = 16.8 Hz, 1H), 2.18 (d, B part of AB system, J = 16.8 Hz, 1H), 2.18 (d, A part of AB system, J = 17.3 Hz, 1H), 2.04 (d, B part of AB system, J = 17.3 Hz, 1H), 1.06 (s, 3H), 9.01 (s, 3H); ^{13}C-NMR (100 MHz, $CDCl_3$) δ 196.7, 167.7, 135.1, 130.6, 130.5, 130.4, 130.2, 127.2, 108.5, 75.9, 51.6, 50.3, 50.0, 41.6, 39.8, 32.4, 29.7, 29.1, 29.9; IR (KBr, cm^{-1})**:** 2922, 2881, 2746, 1769, 1651, 916, 768, 663, 495; HRMS-TOF $[M + H]^+$: Calcd for $C_{18}H_{19}O_2Cl$ 381.0257, found: 381.0258.

5.7 | Reaction of 13 with H_2SO_4

Compound **13** (0.5 g, 1.5 mmol) was treated with a cold solution of conc. H_2SO_4 (20 mL) in MeOH (400 mL). The mixture was heated under reflux for 24 hours. MeOH was evaporated; water (100 mL) was added to the residue and then extracted with CH_2Cl_2. The combined organic layers were washed several times with H_2O, $NaHCO_3$ solution, and dried ($MgSO_4$). The chromatography of the residue (40.0 g) on silica gel eluting with hexane/EtOAc (3:1) gave **17** (0.49 g, (95 %) as the sole product.

5.8 | *rel*-(6*S*(*R*),11*R*(*S*),12*R*(*S*),13*R*(*S*))-13-chloro-11-methoxy-3,3-dimethyl-2,3,4,6,11,12-hexahydro-1H-6,12-methanodibenzo[b,f] oxocin-1-one (17)

Colorless crystals, mp 123 to 125°C; ^{1}H-NMR (400 MHz, C_6D_6) δ 7.10 to 6.95 (m, 4H, arom.), 4.82 (t, J = 2.3 Hz, 1H, H-6), 4.79 (t, J = 2.3 Hz, 1H, H-13), 4.52 (d, J = 2.6 Hz, 1H, H-11), 3.98 (bs, 1H, H-12), 3.41 (s, 3H, OCH_3), 2.03 (dd, A part of AB system, J = 16.1 and 1.5 Hz, 1H, CH_2), 1.72 (dt, A part of AB system, J = 17.1 and 1.5 Hz, 1H, CH_2), 1.92 (dt, B part of AB system,

J = 16.1 Hz, 1H, CH_2), 1.56 (d, B part of AB system, J = 17.1 Hz, 1H, CH_2), 0.78 (s, 3H, CH_3), 0.43 (s, 3H, CH_3); ^{13}C-NMR (100 MHz, C_6D_6) δ 195.3, 166.3, 134.8, 132.3, 130.8, 130.7, 129.6, 128.4, 107.5, 81.8, 76.1, 57.4, 50.5, 50.1, 41.2, 35.3, 31.7, 28.5, 26.5; IR (KBr, cm^{-1})**:** 3045, 2875, 2819, 2647, 2468, 1643, 1438, 874, 657, 531; HRMS-TOF $[M + H]^+$: Calcd for $C_{19}H_{22}O_3Cl$ 333.1257, found: 333.1270.

ACKNOWLEDGEMENT

Financial support from the Turkish Academy of Sciences (TUBA) and Middle East Technical University (METU) is gratefully acknowledged.

REFERENCES

[1] For a reviews on 7-oxabicyclo[2.2.1]heptan intermediates see: a) P. Vogel, J. Cossy, J. Plumet, O. Arjona, *Tetrahedron* **1999**, *55*, 13521; b) P. Chiu, M. Lautens, *Top. Curr. Chem.* **1997**, *190*, 1.

[2] a) Y. Sawama, T. Kawajiri, S. Asai, N. Yasukawa, Y. Shishido, Y. Monguchi, H. Sajiki, *J. Org. Chem.* **2015**, *80*, 5556; b) Y. P. Xue, *J Org Chem* **2011**, *76*, 57; c) Y. Mao, K. M. H. Lim, R. Ganguly, F. Mathey, *Org. Lett.* **2012**, *14*, 4974; d) W.-D. Z. Li, Z.-H. Gao, **2005**, 7, 2917-2920; e) A. Baran, C. Kazaz, H. Secen, Y. Sutbeyaz, *Tetrahedron* **2004**, *59*, 3643; f) M. Koreeda, K.-J. Jung, M. Hirota, *J. Am. Chem. Soc.* **1990**, *112*, 7413.

[3] M. Lautens, S. Ma, *Tetrahedron Lett.* **1996**, *37*, 1727.

[4] a) Y. Huang, C. Ma, Y. X. Lee, R.-Z. Huang, Y. Zhao, *Angew. Chem. Int. Ed.* **2015**, *36*, 13696; b) H. Zhou, J. Li, H. Yang, C. Xia, G. Jiang, *Org. Lett.* **2015**, *17*, 4628; c) E. Carlson, J. Haner, M. McKee, W. G. Tam, *Org. Lett.* **2014**, *16*, 1776; d) C. S. Schindler, S. Diethelm, E. M. Carreira, *Angew. Chem. Int. Ed.* **2009**, *48*, 6296; e) T. Nishimura, T. Kawamoto, K. Sasaki, E. Tsurumaki, T. Hayashi, *J. Am. Chem. Soc.* **2007**, *129*, 1492; f) A. Padwa, Q. Wang, *J. Org. Chem.* **2006**, *71*, 3210; g) M. Lautens, K. Fagnou, S. Hiebert, *Acc. Chem. Res.* **2003**, *36*, 48; h) C. Moinet, J.-C. Fiaud, *Tetrahedron Lett.* **1995**, *36*, 2051.

[5] a) R. Caliskan, N. Nohut, O. Yılmaz, E. Sahin, M. Balci, *Tetrahedron* **2017**, *73*, 291; b) S. Ceyhan, Y. Cetinkaya, A. Akdag, M. Balci, *Tetrahedron* **2016**, *72*, 6815; c) C. Dengiz, R. Caliskan, M. Balci, *Tetrahedron Lett.* **2012**, *53*, 550; d) M. B. Sudemen, M. Zengin, H. Genc, M. Balci, *Turk. J. Chem.* **2011**, *35*, 1; e) M. F. Ali, R. Caliskan, E. Sahin, M. Balci, *Tetrahedron* **2009**, *65*, 1430; f) R. Caliskan, M. F. Ali, E. Sahin, W. H. Watson, M. Balci, *J. Org. Chem.* **2007**, *72*, 3353; g) R. Caliskan, T. Pekel, W. H. Watson, M. Balci, *Tetrahedron Lett.* **2005**, *46*, 6227.

[6] a) M. Mondal, U. Bora, *RSC Adv.* **2013**, *3*, 18716. b) B. B. Snider, *Chem. Rev.* **1996**, *96*, 339.

[7] For the bromination of 3 see: R. Altundas, A. Dastan, M. M. McKee, M. Balci, *Tetrahedron* **2000**, *56*, 6115.

[8] C. Kazaz, A. Dastan, M. Balci, *Magn. Reson. Chem.* **2005**, *43*, 75.

[9] M. Balci, *Basic ^1H and ^{13}C NMR Spectroscopy.* Elsevier: Amsterdam, The Netherlands; **2005**.

[10] Y. Zhao, D. G. Truhlar, *Theor. Chem. Acc.* **2008**, *120*, 215.

[11] C. A. G. Haasnoot, F. A. A. M. DeLeeuw, C. Altona, *Tetrahedron* **1980**, *36*, 2783.

[12] M. J. Frisch, G. W. Trucks, H. B. Schlegel, G. E. Scuseria, M. A. Robb, J. R. Cheeseman, G. Scalmani, V. Barone, G. A. Petersson, H. Nakatsuji, X. Li, M. Caricato, A. Marenich, J. Bloino, B. G. Janesko, R. Gomperts, B. Mennucci, H. P. Hratchian, J. V. Ortiz, A. F. Izmaylov, J. L. Sonnenberg, D. Williams-Young, F. Ding, F. Lipparini, F. Egidi, J. Goings, B. Peng, A. Petrone, T. Henderson, D. Ranasinghe, V. G. Zakrzewski, J. Gao, N. Rega, G. Zheng, W. Liang, M. Hada, M. Ehara, K. Toyota, R. Fukuda, J. Hasegawa, M. Ishida, T. Nakajima, Y. Honda, O. Kitao, H. Nakai, T. Vreven, K. Throssell, J. A. Montgomery Jr., J. E. Peralta, F. Ogliaro, M. Bearpark, J. J. Heyd, E. Brothers, K. N. Kudin, V. N. Staroverov, T. Keith, R. Kobayashi, J. Normand, K. Raghavachari, A. Rendell, J. C. Burant, S. S. Iyengar, J. Tomasi, M. Cossi, J. M. Millam, M. Klene, C. Adamo, R. Cammi, J. W. Ochterski, R. L. Martin, K. Morokuma, O. Farkas, J. B. Foresman, D. J. Fox, Gaussian, Inc., Wallingford CT **2016**.

[13] J. D. Chai, M. Head-Gordon, *Phys. Chem. Chem. Phys.* **2008**, *10*, 6615.

[14] a) A. Klamt, G. Schüürmann, *J. Chem. Soc. Perkin. Trans.* **1993**, *2*, 799; b) J. Andzelm, C. Kölmel, A. Klamt, *J. Chem. Phys.* **1995**, *103*, 9312; c) V. Barone, M. Cossi, *J. Phys. Chem. A* **1998**, *102*, 1995; d) M. Cossi, N. Rega, G. Scalmani, V. Barone, *J. Comput. Chem.* **2003**, *24*, 669.

[15] C. Y. Legault, *CYLview*, 1.0b; Université de Sherbrooke, Sherbrooke, Québec, Canada **2009**. http://www.cylview.org.

SUPPORTING INFORMATION

Additional Supporting Information may be found online in the supporting information tab for this article.

How to cite this article: Çalışkan R, Sari O, Balci M. Functionalization of oxabenzonorbornadiene: Manganese(III)-mediated oxidative addition of dimedone. *J Phys Org Chem*. 2017;30:e3720. https://doi.org/10.1002/poc.3720